Int J. Heat Mass Transfer. Vol. 12, pp. 1231–1248. Pergamon Press 1969. Printed in Great Britain

COUPLED DIFFUSION OF HEAT AND VORTICITY IN A GASEOUS VORTEX

ALAN MIRONER† and DARSHAN S. DOSANJH
Syracuse University, Syracuse, New York

(*Received* 8 *August* 1968 *and in revised form* 7 *March* 1969)

Abstract—This paper describes the coupled diffusion of heat and vorticity in a high temperature, low speed, gaseous vortex. The coupling is caused by both a radial convection of mass resulting from the unsteady heating of the gas and the temperature dependence of the gas properties. The numerical results were obtained by simultaneously solving the fluid heat conduction, continuity, and Navier–Stokes' equations on a digital computer using a finite difference technique. Solutions are presented for two vortex heating situations: (i) initially hot core with cold, irrotational, outer region and (ii) initially cold core with hot, irrotational, outer region. In order to better understand the coupling processes, two gas models are considered: (i) perfect gas with constant thermodynamic and transport properties and (ii) perfect gas with temperature dependent thermodynamic and transport properties. It was found that compressibility increases the rate of vorticity diffusion in the cold core vortex and heat diffusion in the hot core vortex over that of an incompressible vortex. Temperature dependent gas properties further increase the rates of diffusion of both heat and vorticity only in the cold core vortex.

NOMENCLATURE

- a, initial vortex core radius;
- P, pressure;
- Pr, Prandtl number;
- r, radial position;
- R, gas constant;
- t, time;
- T, temperature;
- V_r, radial velocity;
- V_θ, azimuthal velocity;
- Z, compressibility factor.

Greek symbols

- α, numerical stability parameter, $\alpha = \tau/\varepsilon^2$;
- Γ, circulation;
- ε, radial distance grid spacing;
- ζ, vorticity;
- Θ, heat flux potential;
- λ, coefficient of thermal conductivity;
- μ, coefficient of viscosity;
- ν, kinematic viscosity;
- ρ, density;
- σ, coefficient of thermal diffusivity;
- τ, time grid spacing.

Subscripts

- ∞, reference condition for non-dimensionalization (cold properties);
- 0, initial value;
- 1, initial value in core;
- 2, initial value in irrotational region.

INTRODUCTION

HEAT-CONDUCTING vortices are an inherent part of many high temperature gas flow processes such as the exhaust of pulsed jet engines, the blowing of high temperature jet exhaust through leading edge slots on slender delta wings for augmenting lift at low speeds, suspension of nuclear fuels in nuclear rockets, and the stabilization of plasma generators. A periodic, vortex-like structure similar to that occurring in low speed flows is observed in the high temperature wakes of hypervelocity bodies. With this increasing interest in high speed flight and

† Present address: Department of Mechanical Engineering, The Lowell Technological Institute, Lowell, Massachusetts.

other high temperature flow processes, it is becoming very important to understand the behaviour of vortices when large temperature differences and real gas effects are present.

It is well known that both heat and vorticity follow a diffusion-like process when they spread through a medium. Single diffusion processes for a large variety of boundary conditions have been extensively studied and are described in the excellent treatise by Crank [1] on that subject. Deissler [2] has numerically calculated the response of an isolated, incompressible, viscous vortex with an artificially imposed radial velocity present to step changes in both the azimuthal and radial velocities. However, there does not appear to be any work available in which the radial velocity comes about naturally from an unsteady heating process in the gas.

Consider an isolated, rectilinear vortex immersed in an infinite fluid. The vorticity may be considered to be initially uniformly distributed as an instantaneous, cylindrical source. As time passes the vorticity spreads throughout the infinite region following a diffusion process. Now suppose there are also temperature variations present in this flow field which cause heat to spread throughout the region. If the vortex is in a compressible medium, the unsteady density variations caused by the heating introduce a radial velocity which results in a convection of heat and vorticity. And if the temperatures are high enough, real gas effects further affect the diffusion processes by changing the local gas properties.

Two diverse heating situations may be considered. In the first, the core of the vortex is initially hot while the outside, irrotational region is cold. Thus we have a simultaneous, radially outward diffusion of instantaneous cylindrical sources of heat and vorticity. The radial velocity generated by the heating causes an inwardly directed convection of heat and vorticity in the core which opposes the primary diffusion processes. This heating case may be of interest when the vortex cores are formed from the rolling-up of the separated shear/shock heated boundary layer on a high speed projectile.

The second heating case is the reverse of the hot core vortex; i.e., an initially cold core and a hot, outside irrotational region. Here we have a simultaneous, radially outward diffusion of an instantaneous cylindrical source of vorticity, but a radially inward diffusion of heat into a cylindrical sink. The heating generates an outwardly directed radial velocity in the core which convects heat and vorticity in the direction of the primary diffusion of vorticity but opposite to that of the heat. This type of vortex is of interest when the core is formed from cool fluid such as generated by the streaming of a high temperature gas over a cooled, bluff body.

FORMULATION OF THE PROBLEM

Equations

The fluid behaviour is taken to be two-dimensional, unsteady, and axially symmetric. It is assumed that thermal conduction effects predominate over those due to viscous dissipation and compression. This assumption is valid for a not-highly-viscous fluid when the flow velocity and its gradients are small. If in addition, large temperature differences are also present, the assumption of negligible shear and compression heating is even better. A low speed, vortical flow with large temperature gradients meets this criterion very well.

Under the above conditions, the heat conduction equation for a compressible fluid with variable properties written in polar coordinates is

$$\frac{\partial \Theta}{\partial t} + V_r \frac{\partial \Theta}{\partial r} = \sigma \left(\frac{\partial^2 \Theta}{\partial r^2} + \frac{1}{r} \frac{\partial \Theta}{\partial r} \right) \qquad (1)$$

where V_r is the radial velocity and σ is the local thermal diffusivity of the gas. The temperature dependent thermal conductivity has been brought outside the differential operators by using the substitution,

$$\Theta = \int_0^T \lambda(T')\, \mathrm{d}T'$$

to transform the dependent variable from temperature, T, to heat flux potential, Θ.

The continuity equation is

$$\frac{\partial}{\partial t}(\rho r) + \frac{\partial}{\partial r}(\rho r V_r) = 0. \tag{2}$$

The equation of state for a perfect gas with variable composition is

$$P = \rho Z R T \tag{3}$$

where P is the pressure and Z is the compressibility factor which introduces any effects due to changes in chemical composition.

The azimuthal Navier–Stokes equation is

$$\rho\left[\frac{\partial}{\partial t}(rV_\theta) + V_r\frac{\partial}{\partial r}(rV_\theta)\right] = \mu\left[\frac{\partial^2}{\partial r^2}(rV_\theta) - \frac{1}{r}\frac{\partial}{\partial r}(rV_\theta)\right] + \frac{\partial \mu}{\partial r}\left[\frac{\partial}{\partial r}(rV_\theta) - \frac{2}{r}(rV_\theta)\right], \tag{4}$$

where V_θ is the azimuthal velocity.

A fourth equation containing the pressure is now required. Normally, the radial Navier–Stokes' equation would be used,

$$\rho\left[\frac{\partial V_r}{\partial t} + V_r\frac{\partial V_r}{\partial r} - \frac{V_\theta^2}{r}\right] = -\frac{\partial P}{\partial r} + \frac{4}{3}\mu\left[\frac{\partial^2 V_r}{\partial r^2} + \frac{1}{r}\frac{\partial V_r}{\partial r} - \frac{V_r}{r^2}\right] + \frac{2}{3}\frac{\partial \mu}{\partial r}\left[2\frac{\partial V_r}{\partial r} - \frac{V_r}{r}\right].$$

The radial pressure gradient is seen to be influenced by the azimuthal velocity, the radial velocity and its derivatives, and the viscosity and its gradient. It is assumed that we are dealing with low speed (small circulation) vortices, and thus the azimuthal velocity will cause negligible changes in the pressure. Furthermore, we will assume that the radial velocity and its derivatives and the viscosity and its gradient do not appreciably contribute to the radial pressure gradient. The latter assumption must be checked because of the very large temperature gradients in the flow which could conceivably generate substantial radial accelerations and viscosity gradients. Based on these assumptions the density variations are then due mainly to heat conduction/temperature effects; i.e., the effects of dynamics/pressure on the density variation are negligible. We then can assume, for the calculation of the density, that the pressure is constant throughout the flow field. This assumption allows the determination of the temperature, density, and radial velocity to be made independently of the dynamics of the flow. The dynamics, however, are coupled to the preceding results through the density, radial velocity, and temperature dependent gas properties. This one-way uncoupling of the thermodynamics from the dynamics results in a great simplification in the numerical solution.

The vorticity, ξ, is a derived quantity obtainable directly from the azimuthal velocity distribution; i.e., $\xi = (1/r)(\partial/\partial r)(rV_\theta)$

An alternate formulation of the problem would be to derive a vorticity transport equation in which the dependent variable is vorticity rather than azimuthal velocity. This vorticity transport equation must be valid for a compressible fluid with variable viscosity. Solution of this equation would yield the vorticity directly rather than having to first calculate the azimuthal velocity distribution and then use it to calculate the vorticity. It is difficult to tell whether this approach would either reduce the complexity of the numerical solution or increase its accuracy.

Boundary conditions

Boundary conditions for the temperature, radial velocity, and azimuthal velocity must be specified on the $t = 0$ and $r = 0$ axes. Although any initial distribution of temperature and vorticity may be used, a step distribution is used here with the discontinuity occurring at the core edge. The assumption of no sources or sinks of heat at the center of the vortex requires that the first spatial derivative of temperature

at the origin must always be zero. Thus, the required initial conditions for the temperature are:

$$T(r,0) = T_1, \qquad 0 \leqslant \left(\frac{r}{a}\right) \leqslant 1$$

$$T(r,0) = T_2, \qquad \left(\frac{r}{a}\right) > 1 \tag{5}$$

$$\frac{\partial T}{\partial r}(0,t) = 0$$

where a is the initial radius of the vortex core.

Similarly, since there are no sources or sinks of mass at the center of the vortex, the radial velocity at the origin must always be zero. The initial radial velocity may be arbitrarily specified, but to demonstrate the effect of the unsteady heating on its generation, it will be taken as zero. The boundary conditions on the radial velocity are then:

$$V_r(r,0) = V_r(0,t) = 0. \tag{6}$$

The initial azimuthal velocity distribution is taken to be that which results in a vorticity distribution which is uniform and concentrated in the vortex core. The azimuthal velocity at the center of the vortex is always zero. Thus,

$$V_\theta(r,0) = \frac{\Gamma_0}{2\pi a}\left(\frac{r}{a}\right) \qquad 0 \leqslant \left(\frac{r}{a}\right) \leqslant 1$$

$$V_\theta(r,0) = \frac{\Gamma_0}{2\pi a}\left(\frac{r}{a}\right)^{-1} \qquad \left(\frac{r}{a}\right) > 1 \tag{7}$$

$$V_\theta(0,t) = 0$$

where Γ_0 is the initial circulation of the vortex.

The equations of motion and boundary conditions are now non-dimensionalized with respect to initial vortex core radius and initial gas properties occurring in the *cold* region of the vortex. The non-dimensional quantities are denoted by circumflexed symbols, and the subscript, "∞", refers to the reference conditions. The required non-dimensional quantities are:

$\hat{r} = r/a, \hat{t} = t\sigma_\infty/a^2, \hat{T} = T/T_\infty, \hat{\Theta} = \Theta/\Theta_\infty,$
$\sigma = \sigma/\sigma_\infty, \hat{V}_r = aV_r/\sigma_\infty, \hat{\rho} = \rho/\rho_\infty,$
$\hat{V}_\theta = aV_\theta/\sigma_\infty, \hat{\mu} = \mu/\mu_\infty, \hat{Z} = Z/Z_\infty, \hat{P} = 1,$
and $\hat{\xi} = \pi a^2 \xi/\Gamma_0.$

The non-dimensionalized equations of motion are:

heat conduction,

$$\frac{\partial \hat{\Theta}}{\partial \hat{t}} + \hat{V}_r \frac{\partial \hat{\Theta}}{\partial \hat{r}} = \sigma\left(\frac{\partial^2 \hat{\Theta}}{\partial \hat{r}^2} + \frac{1}{\hat{r}}\frac{\partial \hat{\Theta}}{\partial \hat{r}}\right) \tag{8}$$

continuity,

$$\frac{\partial}{\partial \hat{t}}(\hat{\rho}\hat{r}) + \frac{\partial}{\partial \hat{r}}(\hat{\rho}\hat{r}\hat{V}_r) = 0 \tag{9}$$

state,

$$\hat{Z}\hat{\rho}\hat{T} = 1 \tag{10}$$

and azimuthal Navier–Stokes

$$\hat{\rho}\left[\frac{\partial(\hat{r}\hat{V}_\theta)}{\partial \hat{t}} + \hat{V}_r \frac{\partial}{\partial \hat{r}}(\hat{r}\hat{V}_\theta)\right] = Pr_\infty \hat{\mu}\left[\frac{\partial^2}{\partial \hat{r}^2}(\hat{r}\hat{V}_\theta) - \frac{1}{\hat{r}}\frac{\partial}{\partial \hat{r}}(\hat{r}\hat{V}_\theta)\right] + Pr_\infty \frac{\partial \hat{\mu}}{\partial \hat{r}}\left[\frac{\partial}{\partial \hat{r}}(\hat{r}\hat{V}_\theta) - \frac{2}{\hat{r}}(\hat{r}\hat{V}_\theta)\right] \tag{11}$$

where Pr_∞ is the reference Prandtl number.

The simultaneous partial differential equations (8)–(11) with the non-dimensionalized version of the boundary conditions (5)–(7) represent the formulation of the problem of coupled diffusion of heat and vorticity in an isolated, rectilinear, real gas vortex. Since the diffusion processes discussed in this paper deal with a highly non-linear system, the equations describing this problem must be numerically integrated for certain specific examples.

As the gas models become more complex, the generality of the solutions becomes more restricted. In the constant property or ideal gas model, the type of gas is specified only through the reference Prandtl number. This Prandtl number specification is required since the diffusivities for heat and vorticity are related

through the Prandtl number, and the dimensionless time appearing on all the plots is based on the reference thermal diffusivity. The temperature ratio must also be specified, because the magnitude of the radial convection contribution to the overall diffusion process is determined by the temperature/density variations. In the variable property or real gas model, the chemistry of the gas as well as the absolute temperature levels must be specified because of the dependence of the gas properties and density on temperature. We have used the statistical mechanical calculations of Hansen [3, 4] for the high temperature properties of air. Although more recent and possibly more accurate transport property calculations are available, Hansen presents his calculations in a curvefit form which is ideal for use on a digital computer.

It should be noted that both the thermal diffusivity and kinematic viscosity are not constant in the ideal gas model. They change in the ideal gas model because of density variations and change even further in the real gas model because of variations in the thermodynamic and transport properties.

A brief discussion of the numerical integration technique is given in the appendix. A more extensive discussion of the numerical method of solution is contained in the doctoral dissertation of Mironer [5].

RESULTS

The results of the numerical solution of equations (8)–(11) for a specific set of boundary conditions are presented in this section in the form of plots showing the variation of temperature, radial velocity, and vorticity with position and time. Sets of these three plots are presented for each of the two vortex heating cases and for both of the gas models. The radial velocity plots are included for completeness and to indicate the contribution of the radial convection to the overall diffusion processes. Also, crossplots comparing the diffusion processes at the center of the core for the various gas models in both the vortex heating cases are presented.

All quantities have been non-dimensionalized as indicated on each plot. Air is used as the fluid for all calculations. The cold initial temperature is taken to be 500°K which gives a Prandtl number of 0·738. For a vortex having an initial radius of 0·5 cm, and an initial cold region temperature of 500°K, 1 unit of dimensionless time corresponds to about 0·5 sec, and 1 unit of dimensionless velocity corresponds to about 1 cm/s.

In the incompressible, constant property gas model no coupling exists between the heat and vorticity diffusion processes. The results for the diffusion of an initially uniformly distributed, instantaneous cylindrical source in an infinite, constant property, incompressible medium apply for both diffusion processes. Carslaw and Jaeger [6] present a plot for this type of diffusion process using the numerically obtained results of Masters [7]. The curves of the temperature and vorticity at the same times are simply shifted from one another, depending on which diffusivity is used in the non-dimensional time. These plots will not be reproduced here; however, reference will be made to them when discussing the results of the coupled diffusion problem.

In the perfect gas, constant property gas model (ideal gas) results are presented for a 15:1 initial temperature ratio across the vortex. In the perfect gas, variable property gas model (real gas) solutions have been carried out for a 7500°K hot region and 500°K cold region, which is also a 15:1 temperature ratio.

Hot core vortex

Ideal gas model, Figs. 1, 2, and 3. The low density core cools rapidly while the dense, outer gas is heated very little because of the relatively small amount of heat initially contained in the core. The ideal gas model core cools about ten times faster than that of the incompressible vortex. Since the core is cooling and becoming more dense, there must be an inward convection of mass from the outer region to furnish the extra gas required. The outside region in the vicinity of the core edge is receiving

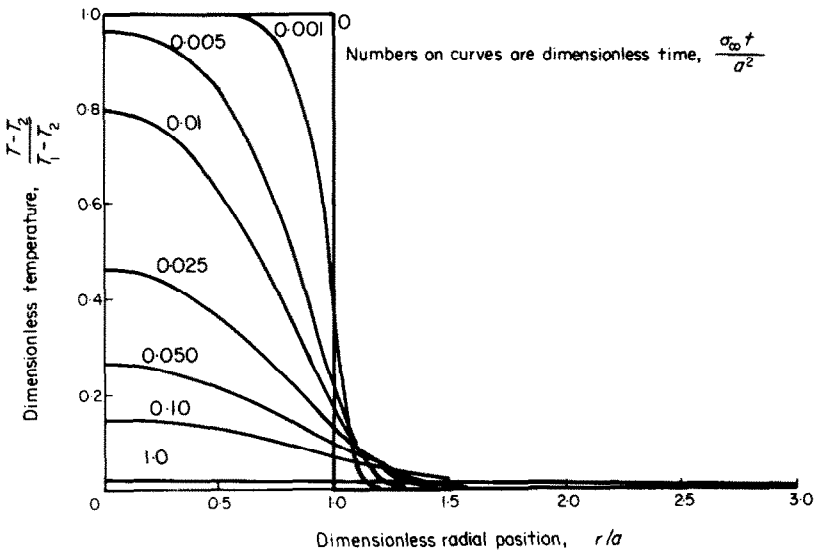

FIG. 1. Temperature history for ideal gas, hot core vortex.
Initial temperature ratio, $T_1/T_2 = 15$.

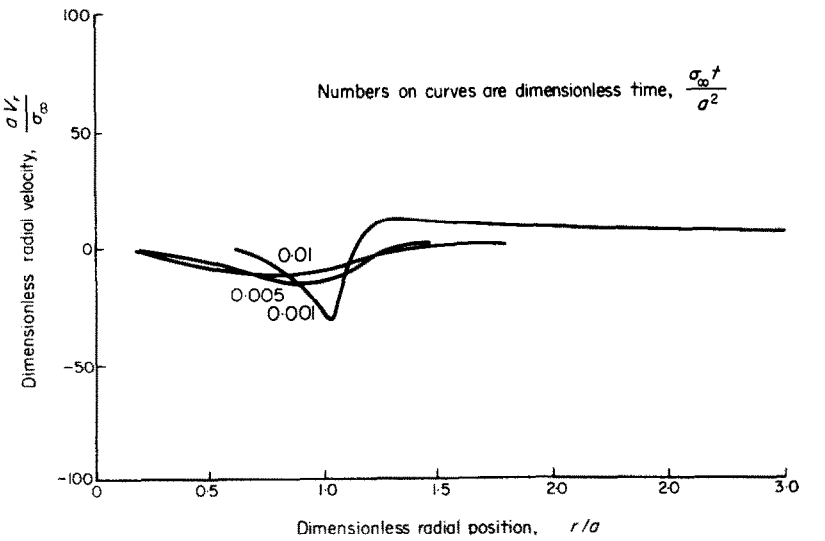

FIG. 2. Radial velocity history for ideal gas, hot core vortex.
Initial temperature ratio, $T_1/T_2 = 15$.

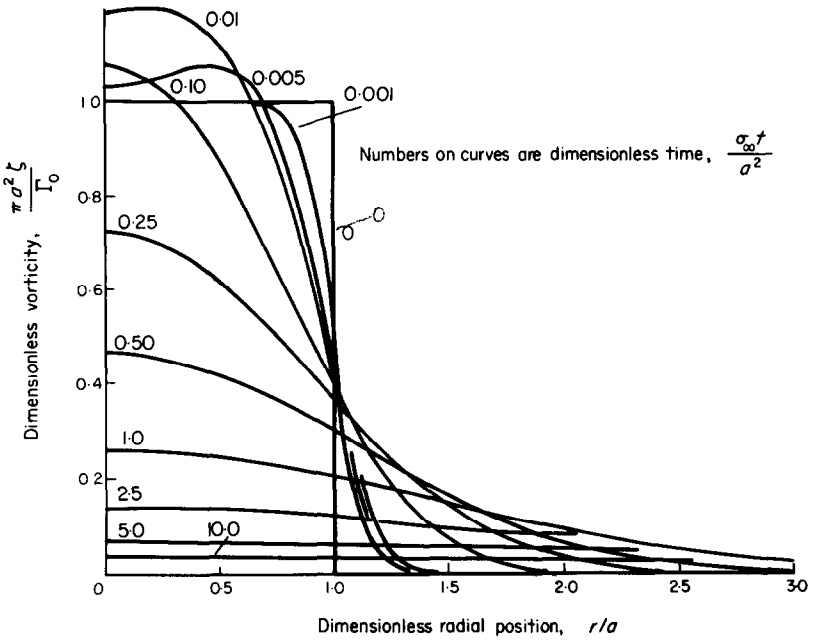

FIG. 3. Vorticity history for ideal gas, hot core vortex. Initial temperature ratio, $T_1/T_2 = 15$; reference Prandtl number, $Pr_\infty = 0{\cdot}738$.

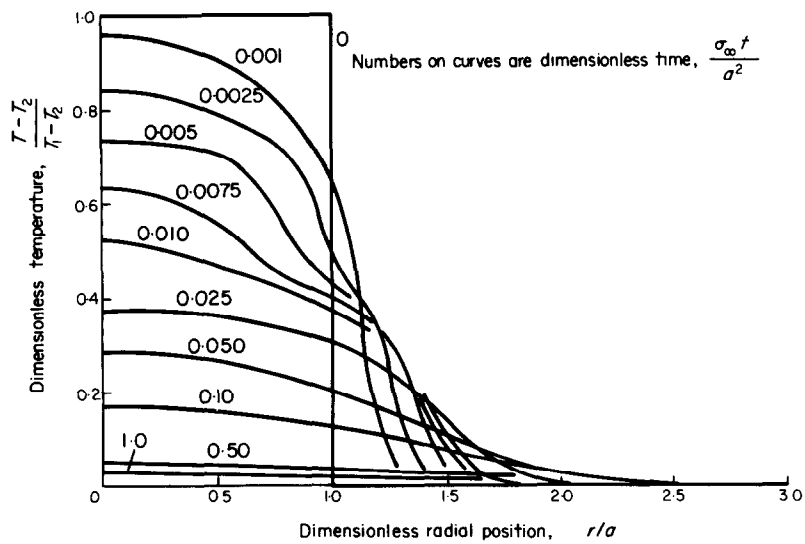

FIG. 4. Temperature history for real gas, hot core vortex. Initial core and outside temperatures, $T_1 = 7500°K$ and $T_2 = 500°K$; gas—air; pressure 1 atm.

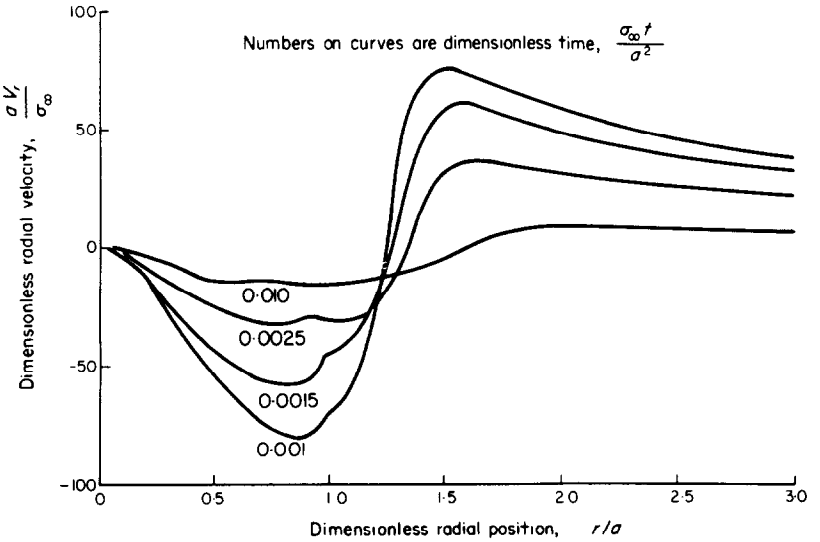

FIG. 5. Radial velocity history for real gas, hot core vortex. Initial core and outside temperature: $T_1 = 7500°K$ and $T_2 = 500°K$; gas—air; pressure—1 atm.

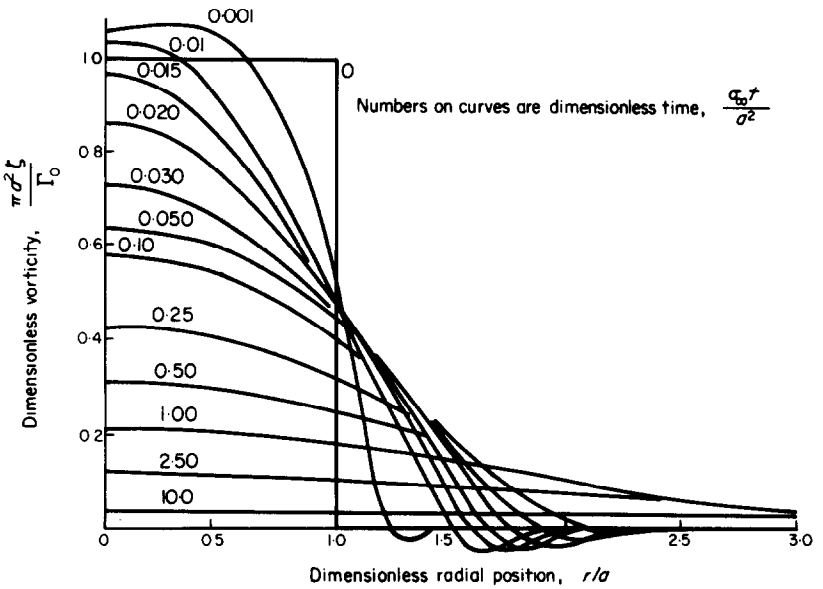

FIG. 6. Vorticity history for real gas, hot core vortex. Initial core and outside temperatures: $T_1 = 7500°K$ and $T_2 = 500°K$; gas—air; pressure—1 atm.; reference Prandtl number, $Pr_\infty = 0{\cdot}738$.

heat from the hot core and its density falls requiring an outwardly directed convection to carry away the excess gas. It will be seen that in both heating cases and for both gas models the radial velocity in the region of the core always opposes the primary diffusion of heat. At large radial distances where the heat diffusion process has not penetrated significantly, the radial velocity has a potential decay. In the beginning of the vorticity diffusion process, the large inwardly directed radial velocity convects vorticity from the outer region of the core into its center and dominates the outwardly directed, primary diffusion. However, as time progresses, the radial velocity decreases, and the primary diffusion process takes over. The initial "pumping" of vorticity into the center of the core and the decreasing kinematic viscosity due to the increasing density slows the overall diffusion of vorticity to the extent that it takes about the same time as that required for completing the vorticity diffusion process in the incompressible vortex.

Real gas model, Figs. 4, 5, and 6. The low density core cools more rapidly in the beginning of the heat diffusion process than the ideal gas core due to the very high value of the thermal conductivity. The thermal conductivity is so high that the temperature gradients are very flat; however, in the outside region, where the conductivity is low, the gradients are quite steep. In the core region the vorticity distribution exhibits the same general behaviour as in the ideal gas solutions; i.e., early in the diffusion process, the very large inwardly directed radial convection results in a net "pumping" of vorticity into the center of the core. The vorticity accumulation in the center of the core is not as large as in the ideal gas vortex due to the counteracting effect of the very high kinematic viscosity in the core which tends to rapidly diffuse the vorticity outward. In the outside region, the vorticity is slightly negative due to the decreased velocity there. The fluid particles in this region are rotating about their centers of mass in a direction opposite to those in the region of positive vorticity, while the centers of mass of all the fluid particles continue to move with an azimuthal velocity of the same direction. The vorticity diffusion process takes about the same length of time as that for the ideal and incompressible gas vortices.

Figures 7 and 8, show comparisons of the core center temperature and vorticity distributions for the three gas models. The incompressible vortex core begins to cool considerably later than either of the compressible vortices and also requires a considerably longer time to cool. The vorticity "pumping" effect is largest for the ideal gas vortex, but due to counteracting mechanisms, all gas models of the hot core vortex require about the same amount of time for the diffusion to be completed.

Cold core vortex

Ideal gas model, Figs. 9, 10, and 11. The dense core heats up very slowly because of the large mass of cold gas in it and the outwardly directed radial convection of heat which opposes the primary, inwardly directed diffusion. It takes about the same time for the core to be heated to near the outside temperature as the incompressible vortex. The vorticity diffuses about ten times faster than in the incompressible vortex because of the outwardly directed radial velocity which augments the primary diffusion and the increasing kinematic viscosity due to the decreasing density.

Real gas model, Figs. 12, 13, and 14. In the early part of the heat diffusion process, the thermal diffusivity is very much lower in the cold core than in the hot, outside region. The low thermal diffusivity acts as a heat insulating mechanism for the core, resulting in very steep temperature gradients. This low thermal diffusivity along with the high density core and the large radial convection which opposes the inwardly directed primary diffusion of heat combine to keep the core temperature low in the beginning of the diffusion process. However, as times passes and the heat penetrates significantly into the core, the thermal diffusivity

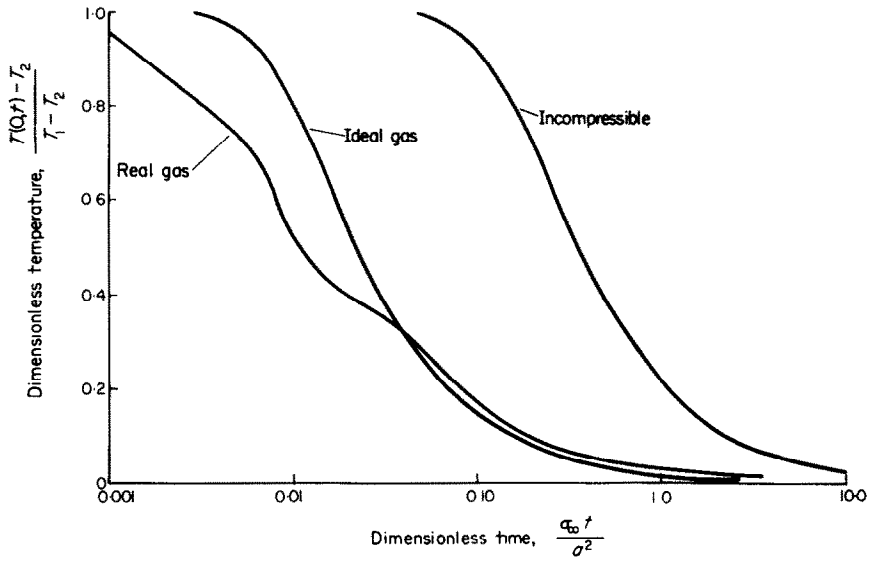

FIG. 7. Comparison of center of core temperature histories in the hot core vortex.

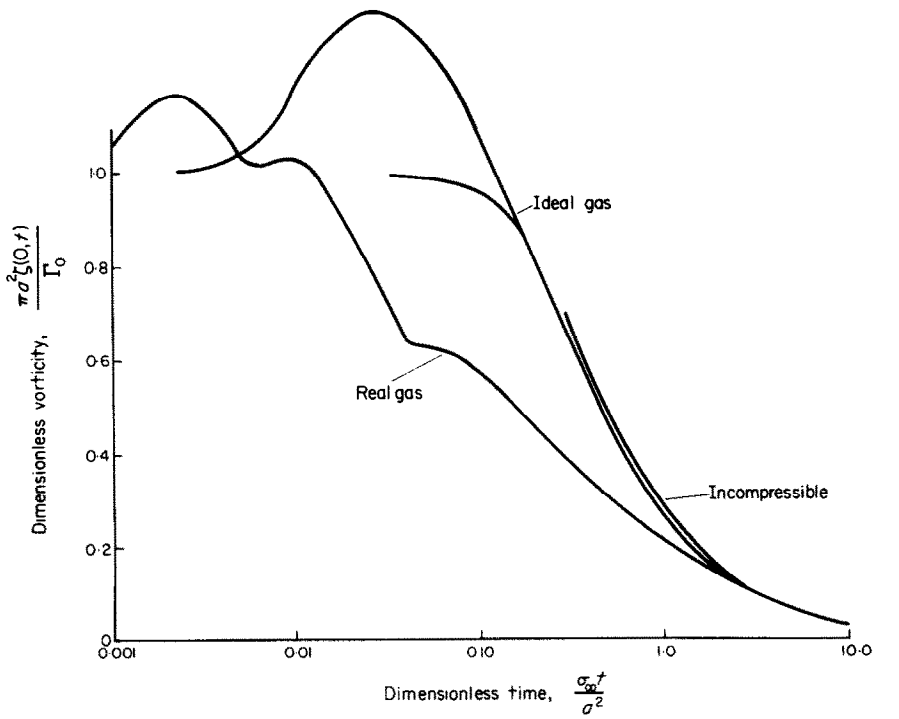

FIG. 8. Comparison of center of core vorticity histories in the hot core vortex.

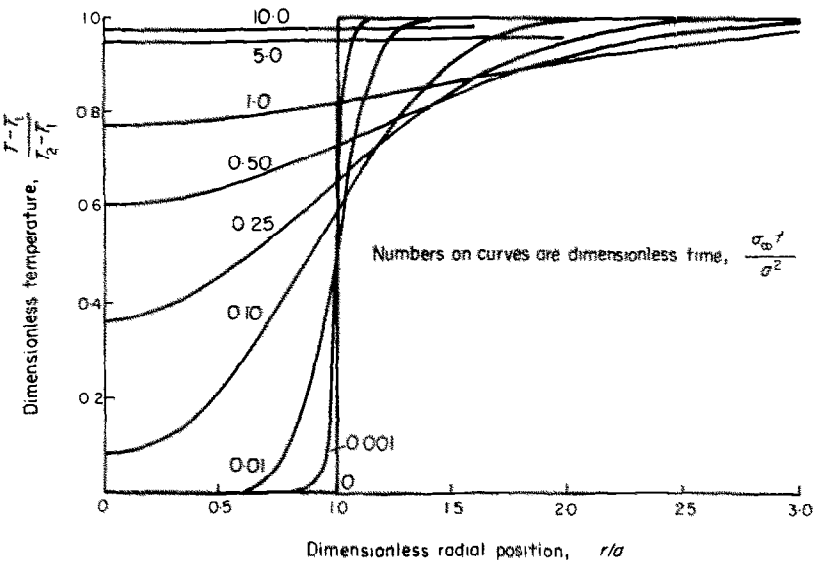

FIG. 9. Temperature history for ideal gas, cold core vortex.
Initial temperature ratio, $T_2/T_1 = 15$.

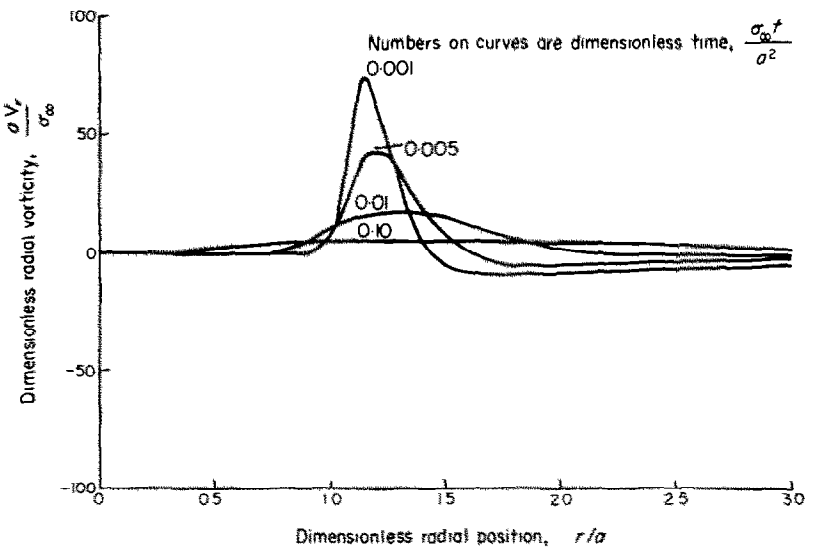

FIG. 10. Radial velocity history for ideal gas, cold core vortex.
Initial temperature ratio, $T_2/T_1 = 15$.

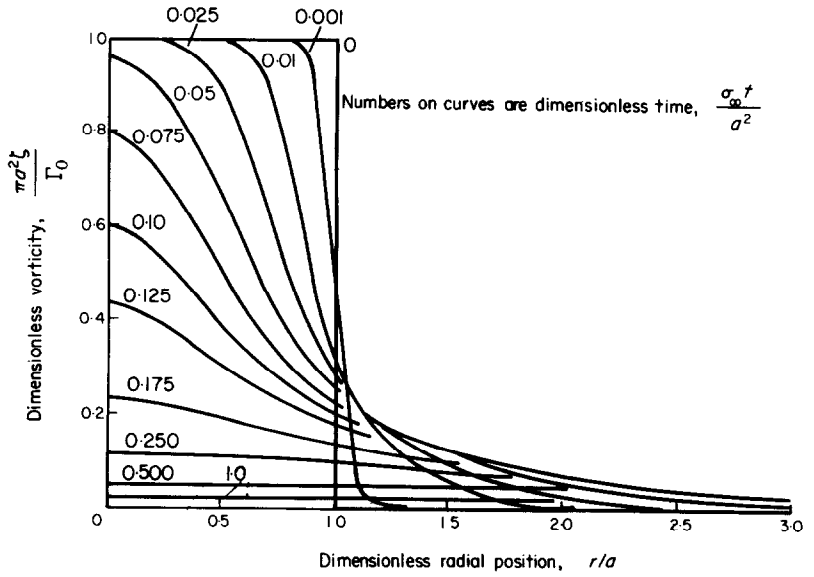

FIG. 11. Vorticity history for ideal gas, cold core vortex. Initial temperature ratio, $T_2/T_1 = 15$; reference Prandtl number, $Pr_\infty = 0{\cdot}738$.

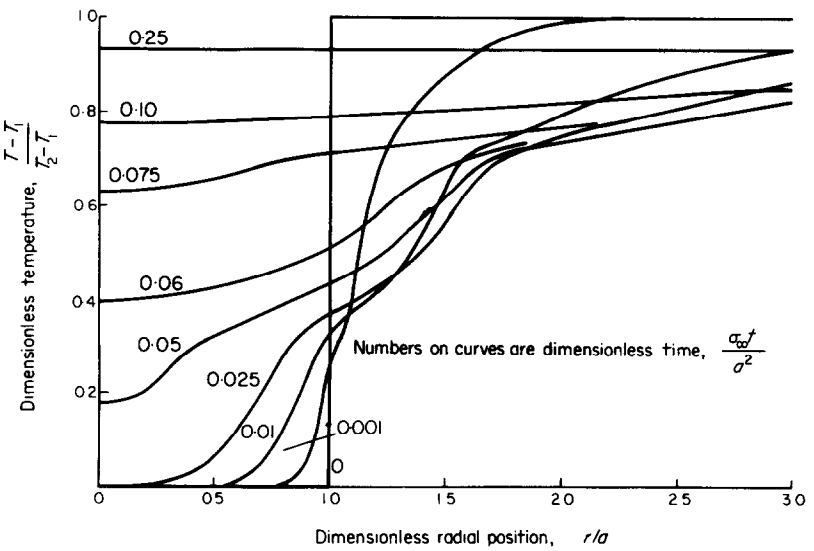

FIG. 12. Temperature history for real gas, cold core vortex. Initial core and outside temperatures; $T_1 = 500°K$ and $T_2 = 7500°K$; gas—air; pressure—1 atm.

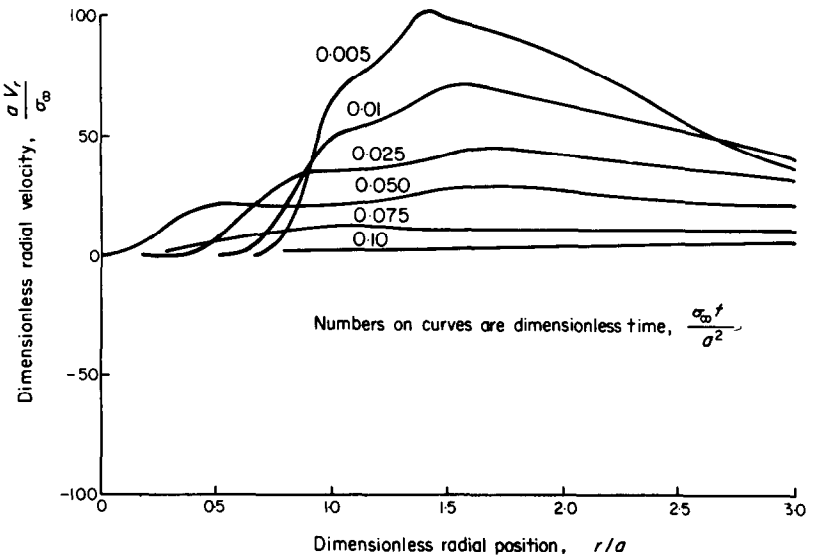

FIG. 13. Radial velocity history for real gas, cold core vortex. Initial core and outside temperatures, $T_1 = 500°K$ and $T_2 = 7500K$; gas—air; pressure—1 atm.

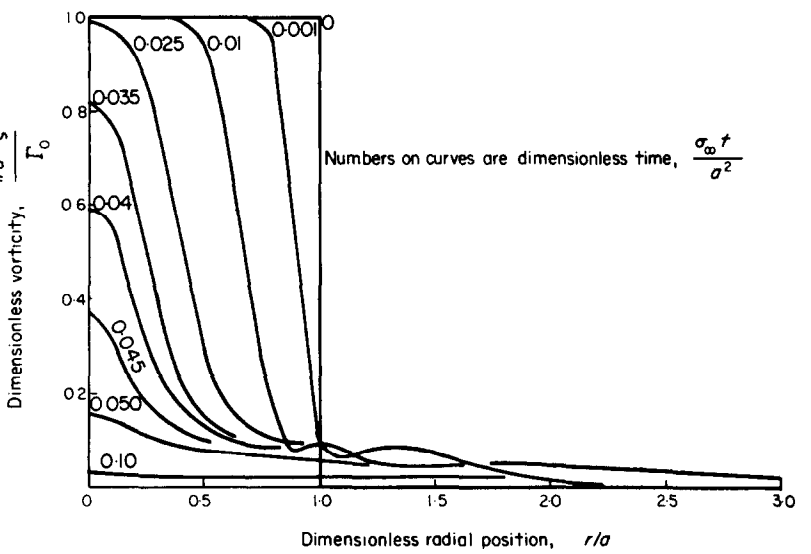

FIG. 14. Vorticity history for real gas, cold core vortex. Initial core and outside temperatures: $T_1 = 500°K$ and $T_2 = 7500°K$; gas—air; pressure—1 atm.; reference Prandtl number, $Pr_\infty = 0{\cdot}738$.

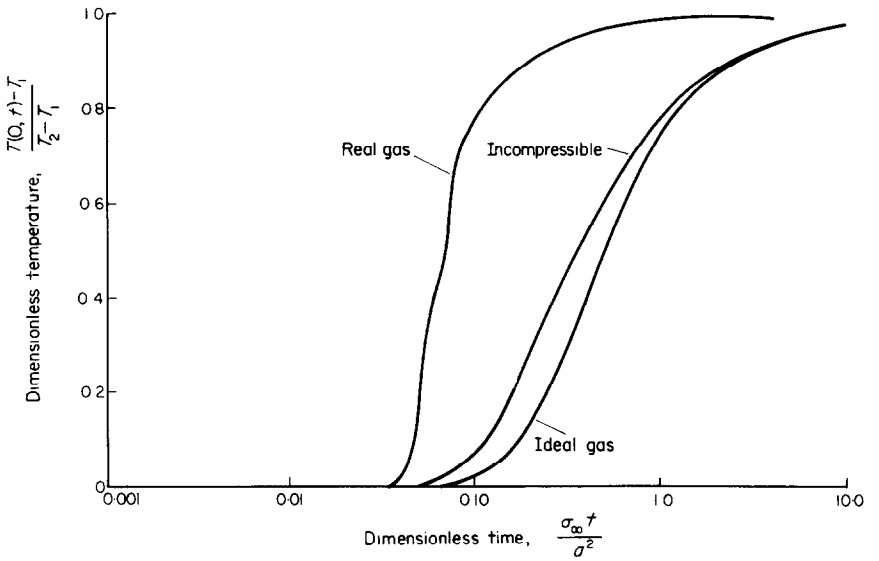

FIG. 15. Comparison of center of core temperature histories for the cold core vortex.

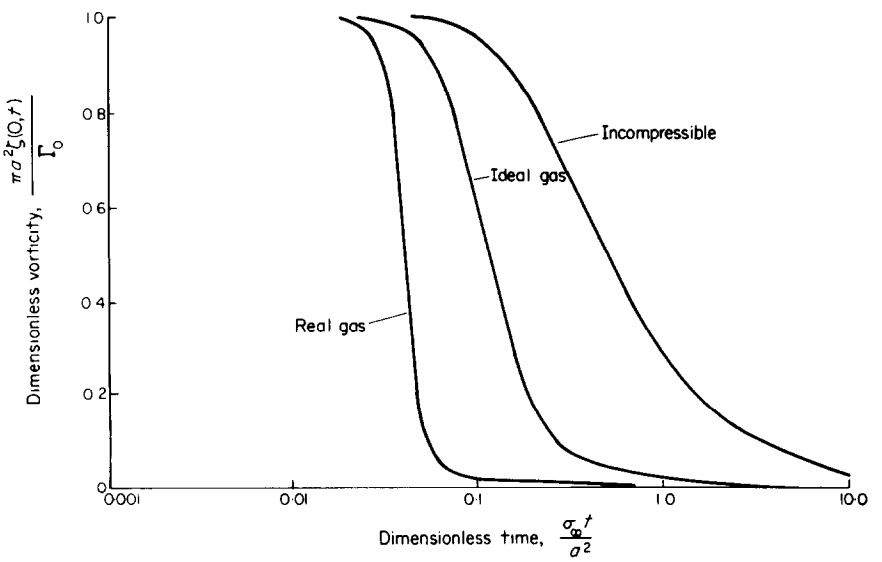

FIG. 16. Comparison of center of core vorticity histories for the cold core vortex.

rises, the density falls, and the radial convection falls off causing the core to heat up faster and faster. The only counteracting mechanism to this accelerated heating of the core is the increasing specific heat which requires increasingly more heat to raise the core temperature by a given amount. The flattening of the temperature (density) gradients in the outside region due to the large thermal conductivity there keeps the radial velocity everywhere outwardly directed. The vorticity diffusion is very much faster than that in the ideal gas model because of the rapidly increasing kinematic viscosity due to the decreasing density and increasing viscosity.

Figures 15 and 16 compare the core center temperature and vorticity distributions for the three gas models. In the ideal gas vortex, the outward radial convection of heat nearly offsets the increase in the core heating rate due to its decreasing density. The rapidly increasing thermal conductivity in the core is the main effect in increasing the heat diffusion rate in the real gas vortex over that of the ideal gas vortex. The separate effects of radial convection and increasing viscosity are shown quite clearly in the vorticity plot.

CONCLUSIONS

The following general conclusions are drawn from the theoretical analysis of a two-dimensional, isolated vortex with moderate circulation and initially large temperature differences between the core and outside regions.

(i) Compressibility substantially increases the vorticity diffusion rate for the cold core vortex and the heat diffusion rate for the hot core vortex, but has little effect on the heat diffusion rate for the cold core vortex and the vorticity diffusion rate for the hot core vortex.

(ii) Temperature dependent gas properties substantially increase the heat and vorticity diffusion rates in the cold core vortex, but have little effect on either diffusion process in the hot core vortex.

The following table summarizes the approximate dimensionless diffusion times associated with the various vortex heating situations and gas models described in this paper.

	Heat diffusion	Vorticity diffusion
Incompressible hot core	10·0	10·0
Ideal gas, hot core	1·0	10·0
Real gas, hot core	1·0	10·0
Incompressible, cold core	10·0	10·0
Ideal gas, cold core	10·0	1·0
Real gas, cold core	1·0	0·1

VALIDITY OF NEGLECTING EFFECTS OF PRESSURE ON DENSITY

The validity of the assumption neglecting the effects of the radial acceleration and viscosity gradients on the pressure gradient has been checked by using the constant pressure distributions of radial velocity, density, and viscosity to calculate the pressure gradient from the radial Navier–Stokes' equation. Using the equation of state, (3), in the form

$$\frac{\Delta\rho}{\rho} = \frac{\Delta P}{P} - \frac{\Delta(ZT)}{(ZT)},$$

the contribution of the temperature/compressibility variation completely dominated the contribution from the pressure variation. Even in the beginning of the diffusion process when the density is changing very rapidly at the edge of the core and generating very large radial velocity changes, the effect of the pressure on the density is negligible.

ACKNOWLEDGEMENT

The authors wish to thank the Syracuse University Computing Centre for use of their facilities and for sponsoring, under NSF Grant GP-1137, the large amount of digital computer computations.

REFERENCES

1. J. CRANK, *The Mathematics of Diffusion*, Clarendon Press, Oxford (1956).
2. R. G. DEISSLER, Unsteady viscous vortex with flow toward the center, NASA TN D-3026 (1965).
3. C. F. HANSEN and S. P. HEIMS, A review of the thermodynamic, transport, and chemical reaction rate properties of high temperature air, NACA TN 4359 (1958).
4. C. F. HANSEN, R. A. EARLY, F. E. ALZOFAN and F. C. WITTEBORN, Theoretical and experimental investigation of heat conduction in air including effects of oxygen dissociation, NASA TR T-27 (1959).
5. A. MIRONER, Vortices and wakes in low speed, thermal plasma flows, Syracuse University, Syracuse, New York. Dissertation (April, 1967).
6. H. S. CARSLAW and J. C. JAEGER, *Conduction of Heat in Solids*, p. 260. Claredon Press, Oxford (1959).
7. J. MASTERS, The p function, *J. Chem. Phys.* **23**, 1865 (1955).
8. B. NOBLE, *Numerical Methods*, Vol. 2, pp. 340–345. Oliver and Boyd, Edinburgh (1964).

APPENDIX

Numerical Solution of Equations of Motion

Finite difference representation

The first step in the simultaneous numerical solution of the differential equations is the replacement of the various differential coefficients by truncated expansions of finite differences. A rather judicious selection of the type of difference expansion must be made in order to ensure a stable numerical solution and also yield the desired quantities for use in the other equations. The stability considerations are discussed in various texts on numerical analysis such as Noble [8].

The scheme of the numerical solution technique is as follows. The time/distance solution space is divided into a rectangular mesh of nodal points in which successive time nodal points are separated by a time, τ, and successive spatial nodal points by a distance, ε. The location of the various nodal points in the solution space is made by the set of coordinates, (m, n), where $\hat{r} = m\varepsilon$ and $\hat{t} = n\tau$.

Since we are dealing with an infinite region, a marching pattern is employed in which by using quantities evaluated at previous nodal points, new quantities are calculated at advanced nodal points. The direction of march is to calculate quantities along a time line (n = constant), moving from the origin outward (m increasing). When all quantities are calculated at all the nodal points possible on that time line, the calculation then proceeds to the next time line, starting once again at the origin and moving outward.

The finite difference representation of the heat conduction equation is obtained by replacing the time derivative by the first term of a forward difference expansion, the first spatial derivative by the first term of a mean difference expansion, and the second spatial derivative by the first term of a central difference expansion. The heat conduction equation then becomes

$$\Theta(m, n+1) = \frac{\alpha}{2}\sigma(m, n) \times \left\{ \left[\left(\frac{2m+1}{m} \right) - \frac{\varepsilon}{\sigma(m,n)} V_r(m,n) \right] \Theta(m+1, n) + \left[\left(\frac{2m-1}{m} \right) + \frac{\varepsilon}{\sigma(m,n)} V_r(m,n) \right] (m-1, n) \right\} + [1 - 2\alpha\sigma(m,n)]\Theta(m,n) \qquad (12)$$

where $\alpha = \tau/\varepsilon^2$ and m, n are integers denoting the coordinates of the various nodal points. For simplicity, the circumflexes have now been dropped, but all quantities are still non-dimensional.

In order to obtain the radial velocity at the desired nodal point and also a stable numerical solution of the continuity equation, the time derivative is replaced by the first term of a forward difference expansion evaluated at the $(m-1, n)$ nodal position and the spatial derivative by the first term of a forward difference expansion evaluated at the $(m-1, n+1)$ nodal position. Solving for the radial velocity at the next spatial nodal point, one obtains

$$V_r(m, n+1) = \left(\frac{m-1}{m} \right) \left\{ \left(\frac{\rho(m-1, n+1)}{\rho(m, n+1)} \right)

$$\times V_r(m-1,n+1)+\left(\frac{\varepsilon}{\tau}\right)\left[\left(\frac{\rho(m-1,n)}{\rho(m,n+1)}\right)-\left(\frac{\rho(m-1,n+1)}{\rho(m,n+1)}\right)\right]\Bigg\}. \quad (13)$$

Finally, the azimuthal Navier–Stokes equation is converted to finite difference form in an exactly similar manner as the heat conduction equation,

$$\begin{aligned}V_\theta(m,n+1) &= \alpha\left(\frac{m+1}{2m}\right)\left[\frac{Pr_\infty}{\rho(m,n)}\left\{\left(\frac{2m-1}{m}\right)\mu(m,n)+\varepsilon\frac{\partial\mu}{\partial r}(m,n)\right\}-\varepsilon V_r(m,n)\right]V_\theta(m+1,n)\\ &+\alpha\left(\frac{m-1}{2m}\right)\left[\frac{Pr_\infty}{\rho(m,n)}\left\{\left(\frac{2m+1}{m}\right)\mu(m,n)-\varepsilon\frac{\partial\mu}{\partial r}(m,n)\right\}+\varepsilon V_r(m,n)\right]V_\theta(m-1,n)\\ &+\left[1-2\alpha\frac{Pr_\infty}{\rho(m,n)}\left\{\mu(m,n)+\frac{\varepsilon}{m}\frac{\partial\mu}{\partial r}(m,n)\right\}\right]V_\theta(m,n), \quad (14)\end{aligned}$$

where

$$\frac{\partial\mu}{\partial r}(m,n)=\frac{\mu(m+1,n)-\mu(m-1,n)}{2\varepsilon}.$$

The vorticity is obtained by using the first term of a mean difference expansion to represent the spatial derivative,

$$\xi(m,n)=\frac{1}{\varepsilon}\left[\left(\frac{m+1}{2m}\right)V_\theta(m+1,n)-\left(\frac{m-1}{2m}\right)V_\theta(m-1,n)\right]. \quad (15)$$

Method of solution

The following order of solution is followed at each nodal point using previously calculated or boundary quantities.

(1) The heat conduction equation, equation (12), is evaluated using values of Θ and V_r from the previous time line to obtain the value of Θ at the new nodal point.

(2) This new value of Θ is converted to temperature using a piecewise straightline fit to the heat flux potential calculations for air from [4].

(3) This temperature is used to obtain σ, μ, and Z using curve-fits developed by Hansen [3].

(4) Z and T are used in equation (10) to obtain ρ.

(5) ρ and previously calculated values of ρ and V_r are used in equation (13) to calculate the new V_r.

This completes the thermodynamics and property calculations at the new nodal point. Now the dynamics are calculated at this point.

(6) Using previously calculated values of V_r, V_θ, and μ in the azimuthal Navier–Stokes equation (14), V_θ is calculated at the new nodal point.

(7) ξ is now calculated from equation (15) using previously calculated values of V_θ.

Stability and accuracy of solution

It can be shown [8] that to ensure stability in the numerical solution of a one-dimensional diffusion type equation without convection, $\alpha < 1/2\sigma$. This requirement is simply extended to variable diffusivity diffusion problems by using the maximum value of the diffusivity occurring in the flow field under consideration. This requirement has been empirically checked in our computer solutions and found to be valid.

In the beginning of the numerical solutions, due to the discontinuity in density, the radial velocity is excessively high and causes the solution to oscillate. In order to overcome this, the radial velocity is artificially suppressed for the first few time lines of the solution until the density discontinuity has sufficiently smoothed out to give a stable solution.

The effect of the mesh size on the accuracy of the solution was studied by calculating solutions for the incompressible gas model in which ε was systematically reduced from 0·5 to 0·05. These solutions were then compared with the plotted results for this gas model given in Carslaw and Jaeger [6] and also with the simple, closed-form solution to the diffusion equation for this gas

model which may be obtained only at the center of the vortex ($r/a = 0$). It was found that $\varepsilon = 0{\cdot}1$ gave excellent agreement and yet did not prohibitively increase the overall calculation time. Based on this comparison, it might not be unreasonable to hope that this accuracy would also extend to the more complicated gas models since the values of the pertinent variables are not changed that drastically from those of the incompressible gas model.

Résumé—Cet article décrit la diffusion couplée de la chaleur et de la vorticité dans un tourbillon gazeux à haute température et à faible vitesse. Le couplage est provoqué à la fois par la convection radiale massique provenant du chauffage instantionnaire du gaz et par la dépendance de la température en fonction des propriétés du gaz. Les résultats numériques ont été obtenus en résolvant simultanément les équations de conduction de la chaleur, de continuité et de Navier–Stokes dans le fluide sur une calculateur numérique en employant une technique de différences finies. Des solution sont présentées pour deux cas de chauffage du tourbillon: 1°) un noyau initialement chaud avec une région extérieure irrotationnelle froide et, 2°) un noyau initialement froid avec une région extérieure irrotationnelle chaude. Afin de mieux comprendre les processus de couplage, deux modèles gazeux sont considérés: 1°) un gaz parfair avec des propriétés thermodynamiques et de transport constantes et 2°) un gaz parfait avec des propriétés thermodynamiques et de transport dépendant de la température. On a trouvé que la compressibilité augmente la vitesse de diffusion de la vorticité dans le tourbillon à noyau froid et de la diffusion de chaleur dans le tourbillon à noyau froid et de la diffusion de chaleur dans le tourbillon à noyau chaud par rapport à un tourbillon incompressible. De plus, la dépendance des propriétés du gaz en fonction de la température augmente les vitesses de difussion à la fois de la chaleur et de vorticité seulement dans le tourbillon froid.

Zusammenfassung—Der Aufsatz beschreibt die gekoppelte Übertragung von Wärme und Drehimpuls in einem Gaswirbel hoher Temperatur und niedriger Geschwindigkeit. Die koppelung entsteht einmal durch die radiale Konvektion auf Grund der ungleichförmigen Erhitzung und zum anderen durch die Temperaturabhängigkeit der Gaseigenschaften. Es wurden numerische Ergebnisse erzielt durch die simultane Lösung der Wärmeleitungs-, der Kontinuitäts- und der Navier–Stokes'schen Gleichungen auf einer digitalen Rechenanlage mit Hilfe einer Differenzenmethode. Es sind Lösungen für zwei Fälle der Aufheizung eines Wirbels wiedergegeben: 1) anfangs ein heisser Wirbelkern mit kalter, nichtrotierender äusserer Schicht und 2) anfangs kalter Wirbelkern mit heisser, nichtrotierender äusserer Schicht. Um die Koppelungsvorgänge besse zu durchleuchten, wurden zwei Gasmodelle betrachtet: 1) ideales Gas mit konstanten thermodynamischen und Transporteigenschaften und 2) ideales Gas mit temperaturbhängigen thermodynamischen und Transport-Eigenschaften. Es zeigte sich, dass die Kompressibilität im Falle des kalten Wirbelkerns die Wärmeübertragung steigert verglichen mit einer Wirbelströmung in einem inkompressiblen Medium. Die Temperaturabhängigkeit der Gaseigenschaften steigert den Transport von Wärme und Impuls nur im Falle des kalten Wirbelkerns.

Аннотация—В статье описывается связанная диффузия тепла и завихренности в высокотемпературном, газовом вихре при малой скорости движения газа. Связь вызывается радиальной конвекцией массы в результате нестационарного нагрева газа и температурной зависимостью свойств газа. Численные результаты получены путем одновременного решения уравнений энергии неразрывности и уравнений Навье–Стокса на цифровой вычислительной машине с помощью метода конечных разностей. Представлены решения для двух случаев вихревого нагрева: (1) первоначально горячее ядро с холодной, невращающейся внешней областью и (2) первоначально холодное ядро с горячей невращающейся внешней областью. Чтобы лучше понять связь процессов, рассматриваются (1) идеальный газ с постоянными термодинамическими свойствами и свойствами переноса и (2) идеальный газ с термодинамическими свойствами и свойствами переноса, зависимыми от температуры. Найдено, что сжимаемость увеличивает скорость диффузии завихренности в вихре с горячим ядром по сравнению с этой скоростью в случае вихра в несжимаемом газе. Зависимые от температуры свойства газа увеличивают скорости диффузии как тепла, так и завихренности только в холодном вихре.